

Published in final edited form as:

*Vis Neurosci.* 2007 ; 24(4): 535–547. doi:10.1017/S0952523807070502.

## Amacrine cell contributions to red-green color opponency in central primate retina: A model study

D.S. LEBEDEV<sup>1</sup> and D.W. MARSHAK<sup>2</sup>

<sup>1</sup>Laboratory of Sensory Information Processing, Institute for Information Transmission Problems, Moscow, Russia

<sup>2</sup>Department of Neurobiology and Anatomy, University of Texas Medical School, Houston, Texas

### Abstract

To investigate the contributions of amacrine cells to red-green opponency, a linear computational model of the central macaque retina was developed based on a published cone mosaic. In the model, amacrine cells of ON and OFF types received input from all neighboring midget bipolar cells of the same polarity, but OFF amacrine cells had a bias toward bipolar cells whose center responses were mediated by middle wavelength sensitive cones. This bias might arise due to activity dependent plasticity because there are midget bipolar cells driven by short wavelength sensitive cones in the OFF pathway. The model midget ganglion cells received inputs from neighboring amacrine cells of both types. As in physiological experiments, the model ganglion cells showed spatially opponent responses to achromatic stimuli, but they responded to cone isolating stimuli as though center and surround were each driven by a single cone type. Without amacrine cell input, long and middle wavelength sensitive cones contributed to both the centers and surrounds of model ganglion cell receptive fields. According to the model, the summed amacrine cell input was red-green opponent even though inputs to individual amacrine cells were unselective. A key prediction is that GABA and glycine depolarize two of the four types of central midget ganglion cells; this may reflect lower levels of the potassium chloride co-transporter in their dendrites.

### Keywords

Midget ganglion cell; Color vision; Parvocellular; Primate; Parafovea

### Introduction

Midget cells are the most common type of ganglion cell in the primate retina. They are also known as P cells because they project to the parvocellular layers of the lateral geniculate nucleus, giving rise to one of the major parallel processing streams (Callaway, 2005). In the central retina, they generally receive an excitatory input from a single midget bipolar cell which, in turn, receives input from a single long (L) or middle (M) wavelength sensitive cone. Midget cells also receive at least half of their input from amacrine cells, local circuit neurons that use the neurotransmitters GABA or glycine (Kolb & Marshak, 2003). One presynaptic amacrine cell has already been identified, a glycinergic, narrow field cell (Kolb et al., 2002), and several other types of amacrine cells are expected to interact with midget ganglion cells based on their morphology (Mariani, 1990; Kolb et al., 1992).

Midget ganglion cells with dendrites in the proximal half of the inner plexiform layer (IPL) have ON responses; they are excited by increments in white light intensity in their receptive field centers and inhibited by that stimulus in the surrounding area. Midget ganglion cells branching in the distal half of the IPL have the opposite, or OFF, responses (Dacey & Lee, 1994). Midget bipolar cells receiving input from short wavelength sensitive (S) cones and presynaptic to midget ganglion cells with OFF responses have been described in macaque retina (Klug et al., 2003), but not in marmoset retina (Lee et al., 2005). This is attributable to a difference between the two species according to a recent anatomical study comparing them directly (Lee & Grünert, 2007).

Electrophysiological studies indicate that most midget ganglion cells within the central retina have responses of opposite polarity to stimulation of the L or the M cones (Dacey & Lee, 1994; Benardete & Kaplan, 1999; Martin et al., 2001; Solomon et al., 2005; Buzás et al., 2006). In the central 6–7°, the input from a single midget bipolar cell is generally assumed to account for the specificity of the excitatory input (Kolb & DeKorver, 1991; Calkins et al., 1994). However, recent reports of electrical coupling between L and M cones (Hornstein et al., 2004) and inputs from multiple midget bipolar cells to central ON midget ganglion cells (Kolb & Marshak, 2003) suggest that more complex circuitry is required to account for the physiological results.

There is a dramatic change in the organization of midget ganglion cell receptive fields with stimuli selective for L or M cones, known as cone isolating stimuli. When receptive fields are mapped with drifting black and white sine wave gratings varying in spatial frequency, the responses at low spatial frequencies are attenuated because the inhibitory receptive field surrounds are stimulated. When the gratings are made using either L or M cone isolating stimuli, however, the same cells respond well at low spatial frequencies, as though there were no antagonistic surround (Kaplan et al., 1988; Shapley et al., 1991). Essentially the same result was obtained using other types of large, cone isolating stimuli (Reid & Shapley, 1992; Smith et al., 1992; Lee et al., 1998; Benardete & Kaplan, 1999). For example, cells with ON responses to white light in the receptive field center and OFF responses to white light in the receptive field surround have ON responses to L cone isolating stimuli and OFF responses to M cone isolating stimuli everywhere in the receptive field.

One interpretation of this result is that the receptive field centers must be driven by a single subtype of midget bipolar cell; this provides strong excitation over a relatively small area, the receptive field center. Neurons driven by the other subtype of cone and midget bipolar cell provide weaker, inhibitory input extending over a larger area, the receptive field surround. According to this “cone specific surround” hypothesis, in the example above, the ON responses to white light in the receptive field center would come from L cones, and the OFF responses to white light in the receptive field surround would come from M cones. Centers and surrounds with selective inputs are optimal to detect differences in color, although this is achieved at the expense of sensitivity to differences in brightness.

All the anatomical evidence indicates that horizontal cells and amacrine cells are unselective in their connections, however, and these findings support the opposite view, known as the “mixed surround” hypothesis (Solomon & Lennie, 2007). Ray Dacheux was the first person to study the light responses of primate horizontal cells using intracellular electrodes, and results of his elegant experiments were critical in the development of the “mixed surround” hypothesis. At the time, it was known from anatomical studies that H1 horizontal cells contacted both L and M cones (Boycott et al., 1987). However, the possibility remained that some dendrites of the H1 cells were presynaptic and others postsynaptic to the cones. Ray and Elio Raviola showed that H1 cells hyperpolarized when stimulated with all wavelengths of light and were not color opponent. They also confirmed that H1 cells were unselective in

their connections with L and M cones (Dacheux & Raviola, 1990). Amacrine cells also receive input unselectively from all the bipolar cells within their dendritic fields (Calkins & Sterling, 1996).

These two sets of results can be reconciled if neural circuits in the IPL are selectively activated by cone isolating stimuli. To address this question, we developed a linear, computational model of the central primate retina that was constrained by anatomical and physiological results. According to the model, two hypothetical types of amacrine cells in the pathway providing input to midget ganglion cells produce responses that are more cone selective than would be predicted from the distribution of L and M cones. Parts of this work have been published previously in abstract form (Lebedev & Marshak, 2006).

## Materials and methods

### Predictions of the “mixed surround” hypothesis

The receptive field profiles of a midget ganglion cell may be approximated by a difference of two Gaussians (Rodieck, 1965):

$$R(x) = \begin{cases} \frac{L_c \cdot C_c}{\sigma_c \sqrt{\pi}} \exp\left\{-\frac{(x-x_c)^2}{2\sigma_c^2}\right\} - \frac{L_s \cdot C_s}{\sigma_s \sqrt{2\pi}} \exp\left\{-\frac{(x-x_s)^2}{2\sigma_s^2}\right\} & \text{for L stimulus} \\ \frac{M_c \cdot C_c}{\sigma_c \sqrt{2\pi}} \exp\left\{-\frac{(x-x_c)^2}{2\sigma_c^2}\right\} - \frac{M_s \cdot C_s}{\sigma_s \sqrt{2\pi}} \exp\left\{-\frac{(x-x_s)^2}{2\sigma_s^2}\right\} & \text{for M stimulus,} \end{cases} \quad (1)$$

where  $x_c$  and  $x_s$  (min of arc) are the coordinates of the receptive field center and surround midpoints, respectively;  $\sigma_c$  and  $\sigma_s$  (min of arc) are a measure of the receptive field center and surround “widths”;  $C_c$  and  $C_s$  (impulses/sec) are responses of the receptive field center and surround to the uniform achromatic full-field stimulus of a given intensity;  $L_c$  and  $M_c = 1 - L_c$  are normalized summed contributions of L and M cones to the receptive field center, respectively;  $L_s$  and  $M_s = 1 - L_s$  are normalized summed contributions of L and M cones to the receptive field surround.

The first and second terms in Eq. (1) describe the responses of the receptive field center and surround, respectively. Formally, the quantity  $R(x)$  may be treated as a response of the ganglion cell to a straight line stimulus as a function of the stimulus line coordinate,  $x$ , although other stimuli are typically used for real measurements of receptive field profiles (Shapley et al., 1991; Croner & Kaplan, 1995; Lee et al., 1998).

In the central primate retina, as a rule, the receptive field center is driven by a single cone of L or M type. Therefore one may expect that  $L_c = 1$  for a cell with L center, or  $M_c = 1$  in the case of M center. But electrical coupling of adjacent cones results in a slight reduction of these values (Hornstein et al., 2004). In accordance with “mixed surround” hypothesis, values of  $L_s$  may vary widely.

In Fig. 1, the function  $R(x)$  is plotted for  $x_c = 3.8$ ,  $x_s = 4.3$ ,  $\sigma_c = 2.1$ ,  $\sigma_s = 5.6$ ,  $C_c = 284$ ,  $C_s = 241$ ,  $L_c = 0.95$ , and  $L_s = 0.4$ .

### Comparison of predicted and real receptive field profiles

The majority of real midget ganglion cells have receptive field centers that respond mainly to stimulation of the cone type that provides input to the presynaptic midget bipolar cell and receptive field surrounds that respond mainly to stimulation of the opposite cone type (Shapley et al., 1991; Lee et al., 1998). The profiles of such cells may be fit with Eq. (1), setting  $L_s \approx 0$  for a cell with L center, or  $M_s \approx 0$  in the case of M center.

For example, the receptive field profiles of a real midget ganglion cell with L center may be approximated as

$$R_L(x) = \begin{cases} \frac{C_c}{\sigma_c \sqrt{2\pi}} \exp\left\{-\frac{(x-x_c)^2}{2\sigma_c^2}\right\} & \text{for L stimulus} \\ -\frac{C_s}{\sigma_s \sqrt{2\pi}} \exp\left\{-\frac{(x-x_s)^2}{2\sigma_s^2}\right\} & \text{for M stimulus,} \end{cases} \quad (2)$$

where  $x_c = 3.8$ ,  $x_s = 4.3$ ,  $\sigma_c = 2.1$ ,  $\sigma_s = 5.6$ ,  $C_c = 284$ , and  $C_s = 241$  (Lee et al., 1998).

Eq. (1) was derived without taking into account the effects of amacrine cells on the ganglion cells. It is reasonable to assume that the difference between the experimental data and the results predicted by the “mixed surround” hypothesis may be explained by additional signals from the amacrine cells to the ganglion cells. In a linear approach, the signal,  $A_L(x)$ , may be treated as additive, i.e.,

$$R_L(x) = R(x) + A_L(x).$$

It follows from Eqs. 1 and 2 that

$$A_L(x) = \pm \left( \frac{M_c \cdot C_c}{\sigma_c \sqrt{2\pi}} \exp\left\{-\frac{(x-x_c)^2}{2\sigma_c^2}\right\} + \frac{L_s \cdot C_s}{\sigma_s \sqrt{2\pi}} \exp\left\{-\frac{(x-x_s)^2}{2\sigma_s^2}\right\} \right). \quad (3)$$

For a ganglion cell with M center the additional signals are

$$A_M(x) = R_M(x) - R'(x),$$

where the functions  $R'(x)$  and

$$R_M(x) = \begin{cases} -\frac{C'_s}{\sigma'_s \sqrt{2\pi}} \exp\left\{-\frac{(x-x'_s)^2}{2\sigma'^2_s}\right\} & \text{for L stimulus} \\ \frac{C'_c}{\sigma'_c \sqrt{2\pi}} \exp\left\{-\frac{(x-x'_c)^2}{2\sigma'^2_c}\right\} & \text{for M stimulus} \end{cases}$$

are similar to Eqs. (1) and (2), respectively, but with other values of the parameters. Thus

$$A_M(x) = \mp \left( \frac{L'_c \cdot C'_c}{\sigma'_c \sqrt{2\pi}} \exp\left\{-\frac{(x-x'_c)^2}{2\sigma'^2_c}\right\} + \frac{M'_s \cdot C'_s}{\sigma'_s \sqrt{2\pi}} \exp\left\{-\frac{(x-x'_s)^2}{2\sigma'^2_s}\right\} \right). \quad (4)$$

The upper signs in Eqs. (3) and (4) stand for the L stimulus and the lower ones stand for the M stimulus. That is, the signal  $A_L(x)$  is positive for the L stimulus and negative for the M stimulus. The signal  $A_M(x)$  is of opposite polarity. Plots of functions  $R_L(x)$  and  $A_L(x)$  are also shown in Fig. 1.

It is evident that the amacrine cells in the circuit providing input to midget ganglion cells should behave as follows. (1) Their receptive field profiles are roughly similar to those of

the ganglion cell surround. (2) Taken together, their light responses are red-green opponent. (3) The polarity of the amacrine cell signal depends on cone type providing input to the center of the post-synaptic ganglion cell. (4) There is no net response to achromatic stimuli, which are the sum of two cone specific stimuli of equivalent intensity.

### A hypothetical amacrine cell network

A hypothetical amacrine cell network generating signals with the required properties may, in principle, be constructed in many different ways. The scheme here was chosen because of its simplicity and its consistency with the known morphological and electrophysiological data from the central primate retina. One constraint was that the amacrine cells receive input from both types of midget bipolar cells. An electron microscopic study of the amacrine cells presynaptic to midget bipolar cells in central macaque retina indicated that they receive input from all the bipolar cells within their dendritic fields (Calkins & Sterling, 1996). Another constraint was that the amacrine cells provide input to both ON and OFF midget ganglion cells (Kolb et al., 2002).

The hypothetical network consists of two subnetworks with equal numbers of cells, one of ON amacrine cells, and the other of OFF amacrine cells. The inputs to the amacrine cells that contact midget ganglion cells in central macaque retina have been studied by serial reconstruction of electron micrographs (Calkins & Sterling, 1996). The number of midget bipolar cells presynaptic to these amacrine cells ranged from 4–10. Because these authors suggested that the reconstructions were incomplete, the highest value was selected for the model. Both model amacrine cell types receive input, on average, from 10 of the closest midget bipolar cells of the same polarity. OFF amacrine cells have slightly greater weights,  $W_M$ , for inputs from M center OFF bipolar cells and slightly lesser weights,  $W_L$ , for those from L center OFF bipolar cells. Conversely, ON amacrine cells have identical weights,  $W_0$ , for the inputs from ON bipolar cells with L and M centers. This weight is less than  $W_M$  and greater than  $W_L$ . Every midget ganglion cell receives signals from 4–5 ON amacrine cells and a similar number of OFF amacrine cells. The L Off and M On ganglion cells receive signals via sign inverting synapses; the L On and M Off cells receive signals via sign conserving synapses. The network is depicted schematically in Fig. 2.

As an example of how the model amacrine cell network contributes to the responses of midget ganglion cells to cone isolating stimuli, consider the L-ON midget ganglion cell. Both ON and OFF amacrine cells make sign conserving synapses onto the L-ON ganglion cell. With an L cone stimulus that increases in intensity, the ON amacrine cell depolarizes and, in turn, depolarizes the L-ON midget ganglion cell. This augments the ganglion cell's response from the L-ON midget bipolar cell. The OFF amacrine cell hyperpolarizes, but because of its bias toward M cones, its signal is smaller than that of the ON amacrine cell. In other words, the net amacrine cell signal is depolarizing with L cone stimulation. With an M cone stimulus increasing in intensity, the L-ON ganglion cell is hyperpolarized by the L-ON midget bipolar cell. This is augmented by a hyperpolarization from the OFF amacrine cell. The ON amacrine cell depolarizes and transmits this depolarization to the L-ON midget ganglion cell, but the signal from the OFF amacrine cell is larger because of its bias toward M cone inputs. In other words, the net amacrine cell signal is hyperpolarizing with M cone stimulation. Thus, with chromatic stimulation, the amacrine cells collectively produce an L-ON/M-OFF response in the L-ON midget ganglion cell.

### A computational model of the midget pathway

A computational model of the midget pathway in the central primate retina was used to test the efficacy of the hypothetical amacrine cell network (Lebedev, 2003). The model consists of five levels: cones, horizontal cells, bipolar cells, amacrine cells and ganglion cells. Inputs

to neurons of a given level are the outputs of the neurons of one or two preceding levels. The model is linear; the output of any neuron is defined as a weighted sum of its inputs. The model is static; that is, only stationary stimuli are used and steady state neuron outputs are calculated.

The types and coordinates of the cones were taken from the description of a fragment of the real cone mosaic of a macaque retina (Roorda et al., 2001). The fragment (Fig. 3) is situated about 1.5 degrees from the center of the fovea, and its size is approximately 0.125 by 0.125 mm, or 36 by 36 min of arc. The density of the cones in the fragment is about 70000 mm<sup>-2</sup>, the average distance between adjacent cones is equal to 4  $\mu$ m, or 1.16 min of arc. In the fragment there are 904 cones, 826 of which are of L and M types. Integer Cartesian coordinates of cones,  $x$ ,  $y$ , were varied from 0 to 255. A unit coordinate step corresponds to about 0.5  $\mu$ m on the retina, or 0.141 min of arc. The receptive field profile of a model cone was approximated by a Gaussian function with  $\sigma_c = 0.8$  min of arc, a value approximately equal to the average distance between cones (Campbell & Gubish, 1966). Each L or M cone was connected with a single pair of ON and OFF model ganglion cells via ON and OFF model bipolar cells. Adjacent cones were coupled electrically, and the strength of coupling was adjusted according to the results of a recent physiological study (Hornstein et al., 2004). In the central macaque retina, S cones contact OFF midget bipolar cells (Klug et al., 2003) which, in turn, contact amacrine cells (Calkins & Sterling, 1996). However, the S cones comprise only 9% of the total in the region selected for analysis, and so, for the sake of simplicity, midget bipolar cells were not connected to S cones in the model. Therefore, OFF amacrine cells in areas of the model retina containing S cones received slightly fewer inputs from bipolar cells than those in other areas.

The model included 470 horizontal cells. Centers of their circular dendritic fields were located at the nodes of a regular triangular lattice. The lattice step was set so that these cells filled the whole mosaic fragment. Each cell received inputs from the nearest 6–7 L and M cones. Because H1 horizontal cells do not contact S cones (Dacey et al., 1996), the model horizontal cells in the vicinity of S cones received slightly fewer inputs from cones than the others. Each horizontal cell was coupled electrically with its closest neighbors. The strength of horizontal cell coupling was adjusted to obtain a 1.5-fold expansion of the receptive field relative to the dendritic field (Packer & Dacey, 2002). Each model bipolar cell received direct input from a single L or M cone type and also an antagonistic, summed signal from the 3–4 horizontal cells that contact this cone.

The connections between model cones, horizontal cells and bipolar cells are depicted in Fig. 4. The parameters of the cone, horizontal cell, and bipolar cell levels of the model were based on published data. A more detailed description of this part of the model was published previously (Lebedev, 2003).

The model included 392 ON and 392 OFF amacrine cells located at nodes of a triangular lattice. The lattice step was set so that these cells filled the whole mosaic fragment. The connections between bipolar, amacrine, and ganglion cells have been described above. The program was written using the TMT PASCAL language (TMT Development Corp.) and implemented using personal computer with a Pentium 4 processor.

## Results

Three sets of computer experiments were performed: (1) Measurements of the profiles of the model ganglion cell receptive fields. (2) Measurements of responses of these cells to stimulation of individual cones. (3) Measurements of responses of these cells to cone specific, full-field stimuli.



### One-dimensional profiles of the model ganglion cell receptive fields

Measurements of the one-dimensional profiles of the model ganglion cell receptive fields were made with a stimulus consisting of a narrow, straight line superimposed on a uniform background. The line runs parallel to the  $Y$  axis. Its luminance,  $I_{st}(x)$ , is constant along the  $Y$  axis and has a Gaussian shape along the  $X$  axis in order to take into account the eye's optical properties, i.e.,

$$I_{st}(x) = \Delta I \cdot \exp\left\{-\frac{x-x_{st}^2}{2\sigma_{st}^2}\right\} + I_0,$$

where  $I_0$  is the background luminance;  $\Delta I$  is the maximal additional luminance of the stimulus line, and  $x_{st}$  is the line position. The line width is determined by the parameter  $\sigma_{st} = 5.67$  coordinate steps ( $2.83 \mu\text{m}$  or  $0.8$  min of arc on the retina). During an experiment, the line moved along the  $X$  axis by coordinate steps of  $0.5 \mu\text{m}$  on the retina, or  $0.141$  min of arc, from  $x_{st} = 24$  up to  $x_{st} = 231$ . At each of 208 line positions, the responses of all the model neurons were computed.

Fig. 5 shows the receptive field profile of one model ganglion cell measured with an achromatic straight line stimulus, which stimulates L and M cones equally. The profile has the shape of a "Mexican hat," as do real midget ganglion cell receptive field profiles (Croner & Kaplan, 1995). By choosing the proper model parameters, it was possible to approximate the model profile by the difference of two Gaussians. Except for the cones, the model neuron receptive field profiles were not assumed to have a Gaussian shape *a priori*; rather they were generated in this form by interactions between neurons in the model.

The other model ganglion cell profiles were of a similar shape, although some of them revealed a considerable asymmetry of the "hat." Due to the irregular arrangement of model horizontal cells relative to model cones, the receptive field surround of a model ganglion cell also had an irregular shape, and its midpoint was sometimes shifted relative to that of the receptive field center. Fig. 5 depicts the receptive field profile with active model amacrine cells and with amacrine cells switched off. It is evident that the model amacrine cells played almost no role in the responses to achromatic stimuli, in accordance with point 4 above. Measurements of other model ganglion cell receptive fields yielded very similar results.

Figs. 6A and 6B show the receptive field profiles of two model ganglion cells with L and M centers measured with cone specific, line stimuli. The responses of the ganglion cells using the full model were compared with those generated without amacrine cells. Profiles with amacrine cells switched off showed spatial opponency in accordance with the "mixed receptive field surround" model (Lennie et al., 1991). That is, cone-specific stimuli that produced excitatory responses when presented in the receptive field center produced inhibitory responses when presented in the receptive field surround. This phenomenon is illustrated by the two negative-going troughs in the response curve on either side of the peak in the center. The profiles of the summed signals from model amacrine cells (crossed curves in Figs. 6A and 6B) have a shape resembling that of the ganglion cell surround profiles

Figs. 6A and 6B also show that the responses to both cone specific stimuli were diminished when amacrine cells were switched off. This decrease in the responses to cone specific stimuli is attributable to the "mixed" receptive field surround as well as to electrical coupling between neighboring cones. In particular, the asymmetric shape of the response to the M cone stimulus in Fig. 6B, when amacrine cells are switched off indicates that the number of M cones surrounding the central cone in the right half of the receptive field

exceeds that in the left half. The increase in the responses to both cone specific stimuli is caused by the summed signals from the model amacrine cells, and this provides evidence for red-green opponency in these signals. A comparison of Fig. 6A and Fig. 6B shows that the summed signals are of the opposite polarity for the ON ganglion cells with L and M centers. Thus, the results of computer experiments depicted in Fig. 5 and Fig. 6 confirm that the proposed amacrine cell network satisfies requirements 1–4 above.

Fig. 6C illustrates the contributions of the model amacrine cells. At first glance, it seems that the ON and OFF signals differ only in sign, but there is actually a slight bias. The negative OFF amacrine cell response to the M cone stimulus is larger in absolute value than the positive ON amacrine cell response. The different polarities of the summed signals from the model amacrine cells for L and M cone specific stimuli are the basis for the red-green opponency transmitted from amacrine cells to ganglion cells. The sum of the signals generated by the model ON and OFF amacrine cells in response to cone specific stimuli are practically equal in amplitude and opposite in polarity and, therefore, color opponent. In response to achromatic stimuli, defined here as stimulating L and M cones equally, the model amacrine cells show no net response, satisfying point 4 above. In the model, the summed signals of the amacrine cells are multiplied by an amplification factor and added to the ganglion cell responses. For a 10% bias, when  $W_M = 1.1 W_0$  and  $W_L = .9 W_0$ , the amplification factor was set as 35 for the model ON ganglion cells with L centers and 33 for those with M centers. The amplification factor values were chosen in the course of computer experiments in order to obtain the maximal gain in red-green opponency while avoiding overcorrection. The values were different for ganglion cells with L and M centers because the L cones were more numerous in this area of the cone mosaic.

The model amacrine cells enhanced the red-green opponency of the majority of model ganglion cells. With a cone specific stimulus that is the same as the stimulus to the receptive field center, the summed signals from the neighboring amacrine cells compensated for the effects of the surrounding cones of the same type. With a stimulus of the opposite type, the signal from the amacrine cells opposed the signal from electrically coupled cones of the same type in the response of the receptive field center. In addition, the signal from the amacrine cells augmented the contribution of the same cones in the response of the receptive field surround.

### Model ganglion cell responses to stimulation of individual cones

To investigate the fine structure of the receptive fields of model neurons, the cones that converge onto model midget ganglion cells and model midget bipolar cells were identified. Each model cone was stimulated by a spot of unit intensity, while the other cones were unstimulated. Then the light spot was moved to the next cone until all 826 cones had been illuminated, in turn. At each spot position, the responses of all the model neurons were computed. Only the responses of ON midget bipolar cells and midget ganglion cells are illustrated; the OFF cells in the corresponding positions had precisely the opposite responses. The numbers for the cones are those assigned by Roorda et al. (2001), and these were used for the corresponding midget bipolar cells and midget ganglion cells, as well.

In Fig. 7 and Fig. 8, the results of these experiments for cells #413 and #870, the same ones shown in Fig. 6, are depicted. Fig. 7A and Fig. 8A illustrate the receptive field structure of two model bipolar cells which are presynaptic to ganglion cells #413 and #870, respectively. These are the same as the responses of model ganglion cells without amacrine cell inputs. The bipolar cells and ganglion cells without amacrine cell input appeared to have “mixed surrounds.” That is, nearly all L and M cones which form the receptive field surround, cones within 3–4 inter-cone distances, inhibited the bipolar cells. Fig. 7B and Fig. 8B show the receptive field structure of the same ganglion cells taking into account the influence of



signals from the amacrine cells. In Fig 7B, depicting a ganglion cell receiving direct input from a bipolar cell driven primarily by an M cone, nearly all M cones from the receptive field surround of the ganglion cell were excitatory, making the receptive field surround “cone specific.” This change in the polarity of the responses to M cones was attributable to signals from the amacrine cells. Likewise, Fig. 8B indicates that all L cones in the receptive field provide excitatory input to a ganglion cell receiving input from a bipolar cell with its major input from an L cone. Thus, each model mid-ganglion cell received a major excitatory input from one cone and several smaller excitatory inputs from nearby cones of the same chromatic type.

Another conclusion following from experiments like those depicted in Figs. 7 and 8 are that the shapes of the bipolar cell and ganglion cell receptive fields were irregular. The S cones were one source of the irregularity because they did not provide input to any of the model neurons. The shapes of the bipolar cell receptive fields reflected slight irregularities in the arrangement of model horizontal cells relative to cones and bipolar cells and the assumption in the model that all connections between cones and horizontal cells as well as between horizontal cells and bipolar cells have equal weights. The receptive field of the bipolar cell was transmitted to the postsynaptic ganglion cell, and the amacrine cells also influenced the shape of the ganglion cell receptive field. The contributions of the amacrine cells reflected the local pattern of clustering of the L and M cones.

### Model ganglion cell responses to uniform, full-field stimuli

The stimuli used to quantify the red-green opponency of the model ganglion cells were L or M cone specific, full-field and uniform. For example, the L cone specific full-field uniform stimulus was equivalent to simultaneous illumination of all L cones by small light spots in the experiments described in the preceding section. The improvement in red-green opponency due to the influence of signals from the model amacrine cells was quantified by calculating an index based on the responses to L and M cone specific stimuli.

Let  $R_{\text{cnt}}$  be a response of a ganglion cell to a cone specific, full-field uniform stimulus selective for the same cone type that provides input to the presynaptic mid-ganglion bipolar cell, the central cone, and  $R_{\text{sur}}$  be a response to a similar stimulus of the opposite cone type. The normalized difference of these responses gives the degree of red-green opponency ( $RGO$ )

$$RGO = \frac{R_{\text{cnt}} - R_{\text{sur}}}{R_{\text{max}}}$$

where  $R_{\text{max}}$  is the maximal response of the receptive field center when cone electrical coupling is absent, serves as an index of red-green opponency. Higher values of  $RGO$  correspond to greater red-green opponency, and the maximal value of  $RGO$  is about 2. Fig. 9 shows the distribution of the measured values of  $RGO$  for 204 model ganglion cells from the central part of the cone mosaic fragment. When amacrine cell signals were switched off (left histogram, light grey), the mean value of  $RGO$  was 0.68 (SD = 0.12), that is, less than 35% of the maximal value. With active amacrine cells (right histogram, dark grey), the mean value of  $RGO$  was 1.7 (SD = 0.21). However, some of the model mid-ganglion cells showed very little red-green opponency, even with amacrine cell input. According to the “mixed surround” hypothesis, these would occur when the ganglion cell is surrounded by ganglion cells driven by cones of the same type. In the model, there was a weak ( $R = -0.38$ ), but significant ( $p < 0.0001$ ) negative correlation between the  $RGO$  of a given model ganglion cell and the number of nearest neighboring cones of the same type as the central

one Selected examples are included in Table 1, and the entire dataset is provided in Supplemental Materials.

Ganglion cell #524 (see Fig. 10), whose central cone is of L type surrounded by three L cones, one M cone, and two S cones, had the weakest opponency (ranking = 1) of the 204 cells,  $RGO = 1.09$ . Among the 25 cells with the lowest values of  $RGO$ , only 6 cells, #392, #246, #577, #391, #510, and #201 had central cones surrounded by cones of the same type. Cells #432 (ranking = 43), #336 (ranking = 68), and #195 (ranking = 87) whose central cones were also surrounded entirely by cones of the same type, had modest, but larger values of  $RGO$ , 1.52, 1.63, and 1.68, respectively. Three other such cells, #537 (ranking = 103), #719, (ranking = 115), and #525 (ranking = 158), even have values of  $RGO$  in the second half of the list (ranking > 102). There were three cells in the sample which had all cones of the opposite type as nearest neighbors: #199, #162, and #249. These cells had a rather modest values  $RGO$ , respectively, 1.61 (ranking = 64), 1.71 (ranking = 96), and 1.73 (ranking = 111). On the other hand, cell #603, showing the strongest opponency ( $RGO = 2.05$ ), had only a single cone of the type opposite to the central cone among its nearest neighbors. The same was true for cone #388 ( $RGO = 2.04$ ).

The discrepancy between the results of the simulations and the predictions based on the nearest neighboring cone type can be explained by taking into account the contributions of the other cones nearby. For example, ganglion cell #388 with an M center has only one L cone, #748, that is a nearest neighbor of the central cone. In Fig. 10, this cone is marked with white digits. Its contribution in the response of the cell to an L cone specific full-field uniform stimulus of unit intensity is only 0.112. The other 29 L cones in the receptive field, the cones surrounding the nearest neighbors of the central cone, contribute 0.797.

### Alternative connectivity schemes for the model amacrine cells

A key assumption in the model was that OFF amacrine cells were more sensitive to inputs from M cones than inputs from L cones. Without this bias in OFF amacrine cell spectral sensitivity, the results were the same as they were without any amacrine cells at all. That is, the inputs from the two types of amacrine cells to the model ganglion cell typically cancelled one another, and the mean value of  $RGO$  was 0.68. A second assumption in the model was that the midget ganglion cells all received input from both ON and OFF amacrine cells. With input from only a single type of amacrine cell, there is only a slight improvement in  $RGO$  because the amacrine cell input to the model ganglion cells is not red-green opponent. The  $RGO$  of some model ganglion cells improved with sign conserving input from these amacrine cells and others with sign inverting amacrine cell input. When the polarity of the synapse between amacrine cells and ganglion cells was optimized for each ganglion cell, the mean value of  $RGO$  was 0.77, that is, a gain of 13%. When ON amacrine cells inhibited only ON midget ganglion cells and OFF amacrine cells inhibited only OFF midget ganglion cells, the amacrine cell signal always opposed that of the bipolar cell. In that case the mean value of  $RGO$  was only 0.62, worse than the performance without any amacrine cells at all. In addition, there was more spatial opponency in response to chromatic stimulation rather than less, as observed in the original model and in physiological experiments. There are many alternative schemes for connecting the amacrine cells, but they all converge on one of the two alternatives described above.

### Discussion

The responses of the model ganglion cells to cone specific stimuli were very similar to those observed in electrophysiological experiments with midget ganglion cells (Kaplan et al., 1988; Shapley et al., 1991; Lee et al., 1998; Reid & Shapley, 1992; Benardete & Kaplan, 1999). According to the model, every ganglion cell received red-green opponent signals

from several adjacent amacrine cells, and this generated responses that were more cone specific than would be predicted from the cone mosaic. At first glance, the model appears to contradict the results of Calkins and Sterling (1996), which showed that amacrine cells are unselectively connected with all bipolar cells within their dendritic fields and therefore not color opponent. However, individual model amacrine cells were not red-green opponent themselves (see Fig. 6C). Instead, the red-green opponency is a property of the summed signals of ON and OFF amacrine cells.

The model has a number of limitations, however. At present, the S cones simply occupy space and are not connected to second order neurons. In the future, H2 horizontal cells, blue cone bipolar cells, small bi-stratified ganglion cells and, possibly, other types of neurons will be added (Calkins, 2001). In addition, the model was static and did not reproduce any of the temporal properties of midget ganglion cell responses. A model of the primate retina developed recently by Momiji et al. (2006, 2007) did this quite well, but it differs from the model described here in a number of other respects. In particular, Momiji et al. use a regular hexagonal arrangement of cones instead of using data from a real primate retina. The next version of the model should incorporate the best features of both approaches. Finally, an assumption underlying the present model is that signals to midget ganglion from the L and M cones sum linearly. However, it has been shown previously that there are nonlinear components in the interactions between L and M cones (Benardete & Kaplan, 1999). More realistic cells and synapses in future versions of the model should be able to reproduce these interactions.

### Chromatic bias in light responses of amacrine cells

OFF amacrine cells receiving synapses from all midget bipolar cells, but with a bias toward those receiving input from M cones, were a key feature of this model. Another recent modeling study demonstrated how this bias toward M cones might develop due to activity dependent synaptic plasticity (Maximov et al., 2006). Their model consisted of three arrays of cells (1) coupled cones based on the same cone mosaic used in this study, (2) OFF midget bipolar cells that each received input from one cone, and (3) OFF amacrine cells that received input from all bipolar cells within their dendritic fields. A series of random, colored stimuli were presented, and the weights of synapses from bipolar cells to amacrine cells were modified using a physiologically plausible, Hebbian-like learning rule depending on the membrane potentials of the presynaptic and postsynaptic neurons (Abbott & Nelson, 2000). Because the difference between the spectral sensitivity functions of L and S cones is greater than the difference between the spectral sensitivity functions of M and S cones, excitatory synapses from bipolar cells with input from M cones were strengthened. These interactions would occur only in the OFF pathway because there is no ON midget bipolar cells receiving input from S cones (Klug et al., 2003). The dendrites of ON midget ganglion cells stratify higher in the IPL than the axons of ON bipolar cells that receive S cone inputs and, presumably, so do the amacrine cells that provide input to midget ganglion cells (Kouyama & Marshak, 1992). In the model retina, the ON amacrine cells were unbiased, but in the real retina, they might respond preferentially to stimulation of L cones, typically the most numerous types in macaque retinas (Deeb et al., 2000; Roorda et al., 2001). If so, there would be even more red-green opponency in the signals originating from the amacrine cell network.

There is anatomical evidence consistent with the model prediction that some bipolar cell synapses in the macaque IPL are stronger than others. According to one group, there are two types of midget bipolar cells in the central retina, one with about 50 synaptic ribbons, one with about 30 synaptic ribbons and very few with values in between. These are found in both the ON and the OFF sublaminae of the IPL (Calkins et al., 1994). At typical dyad synapses in the central primate retina, there are two postsynaptic processes opposite the

ribbon, one amacrine cell dendrite and one midget ganglion cell dendrite (Dowling & Boycott, 1966). Presumably those bipolar cells with 50 synaptic ribbons provide more input to the amacrine cells at their dyad synapses. According to the model, the midget bipolar cells with 50 ribbons would be the L-ON type in the ON sublamina and the M-OFF type in the OFF sublamina. However, another group found a unimodal distribution of synaptic ribbons in central macaque midget bipolar cell terminals (Jusuf et al., 2006). There is also evidence from human psychophysics for plasticity in red-green opponency. The wavelength identified as neutral yellow changes when observers wear red or green filters over one eye. The finding that interocular transfer of the effect is incomplete suggests that some of the underlying changes take place at sites before signals from the two eyes converge in the primary visual cortex, possibly in the inner retina (Neitz et al., 2002).

### **Depolarizing ganglion cell responses to amacrine cell neurotransmitters**

Another key feature of the model is that some midget ganglion cells respond to amacrine cell neurotransmitters with depolarization rather than hyperpolarization. Responses like these have been described in other neurons in the adult central nervous system. Depolarizing responses to GABA and glycine are observed when there are relatively low levels of the potassium chloride co-transporter (KCC2) in the dendrites (Marty & Llano, 2005). Depolarizing responses to GABA and glycine are seen in all cells during early retinal development (Vu et al., 2000). They might be retained selectively in adult L-ON and M-OFF midget ganglion cells as a result of spike timing dependent plasticity (Dan & Poo, 2004). Presumably, this requires nearly simultaneous presynaptic and postsynaptic action potentials at amacrine cell synapses onto midget ganglion cells. There have been no published recordings from the amacrine cells presynaptic to midget ganglion cells, but it is likely that they have spike-like components in their light responses. The best characterized narrow field amacrine cells in mammals, AII cells, depolarize transiently at the onset of their light responses; this is true in several species, including macaques (Dacey, 1999). In rats, a voltage dependent sodium conductance sensitive to tetrodotoxin generates this depolarization (Boos et al., 1993).

According to the model, nearly simultaneous pre- and postsynaptic spikes are more likely to occur at synapses where the amacrine cell and the ganglion cell receive strong input from the same type of bipolar cell. These include synapses from ON amacrine cells onto L-ON midget ganglion cells and also OFF amacrine cell synapses onto M-OFF midget ganglion cells. There is a precedent for this type of spike timing dependent plasticity in the hippocampus. When presynaptic and postsynaptic action potentials occur within 20 ms. at GABAergic synapses, the synapses are modified in the same way as the amacrine to ganglion cell synapses in the model. In hippocampal slices or cultures of hippocampal neurons, coincident spiking leads to a reduction in KCC2 activity in the postsynaptic cell and a shift in the reversal potential of the synaptic current in the depolarizing direction (Woodin et al., 2003). If interactions like these occurred repeatedly during retinal development, the result would be a subset of midget ganglion cells with depolarizing responses to GABA and glycine.

The model could also be implemented using only hyperpolarizing responses to GABA and glycine. In that case, the model amacrine cells would make synapses directly onto L-OFF and M-ON midget ganglion cells. However, another amacrine cell would be interposed at the synapses onto L-ON and M-OFF midget ganglion cells, and the amacrine cells would exert their effects there by reducing inhibition. A similar pattern of synaptic inputs onto an ON-OFF DS ganglion cell has been described in rabbit retina (Dacheux et al., 2003). Synapses between amacrine cells are common in the pathway providing input to midget ganglion cells (Calkins & Sterling, 1996; Kolb & Marshak, 2003). Indeed, synapses between

amacrine cells are the most common type of synapse in the primate IPL (Koontz & Hendrickson, 1987).

### Convergence of cones onto midget ganglion cells

There was considerable convergence of cones onto the model midget ganglion cells, a phenomenon also observed in electrophysiological experiments on macaque midget ganglion cells and their targets in the Ign (Lee, 2003). There are central and smaller, lateral peaks in the sensitivity profiles of many central midget ganglion cells, a finding suggesting that there are multiple excitatory inputs to central midget ganglion cells (de Monasterio & Gouras, 1975). These authors proposed that the lateral peaks originated from amacrine cells rather than gap junctions between neighboring cones. Stimulation of central macaque retinal ganglion cells with chromatic gratings reveals midget ganglion cells whose receptive field centers receive input from both L and M cones (Kaplan et al., 1988). Midget ganglion cells, including those with receptive fields in the central fovea, show a preference for one orientation, a finding suggesting that the receptive fields are elliptical. Because cone receptive fields are circular, this finding suggests that there are inputs from multiple cones (Smith et al., 1990; Passaglia et al., 2002).

Because there is very little, if any, convergence of midget ganglion cells onto cells in the parvocellular layers of the lateral geniculate nucleus (P cells), studies of central P cells are also relevant. Based on responses of P cells to very fine gratings generated by laser interferometry, McMahon et al. (2000) proposed that central midget ganglion cells receive a major input from one cone and smaller inputs from neighboring cones. They also argued that coupling between cones makes a relatively small contribution to this convergence of cone signals onto midget ganglion cells and suggested that amacrine cells make the major contribution.

The results using this model were consistent with these predictions. The responses of model midget bipolar cells were derived solely from interactions in the outer plexiform layer, including cone coupling, and they showed a relatively small amount of convergence. Even though the model midget ganglion cells received input from only one midget bipolar cell, there was considerably more convergence in their responses because they received input from the model amacrine cells. All neighboring cones of the same chromatic type also provided excitatory input, and in some ganglion cell responses, the cones in the rings surrounding the nearest neighbors also made a large contribution. According to the model, the amacrine cells were largely responsible for both the cone selectivity and the large sizes of the receptive fields.

### Conclusions

Signals from amacrine cells enhanced the red-green opponency of model midget ganglion cells, compensating for the “mixed” receptive field surround of midget bipolar cells and the existence of electrical coupling between L and M cones. The model predicts that increasing red-green opponency is one important function of amacrine cells in the pathway providing input to midget ganglion cells in the primate retina.

### Acknowledgments

Supported by grant NS38310 from the National Institute for Neurological Diseases and Stroke. We are grateful to Dr. Stephen Mills for a critical reading of the manuscript and to Dr. Alice Chuang for assistance with the statistical analysis.



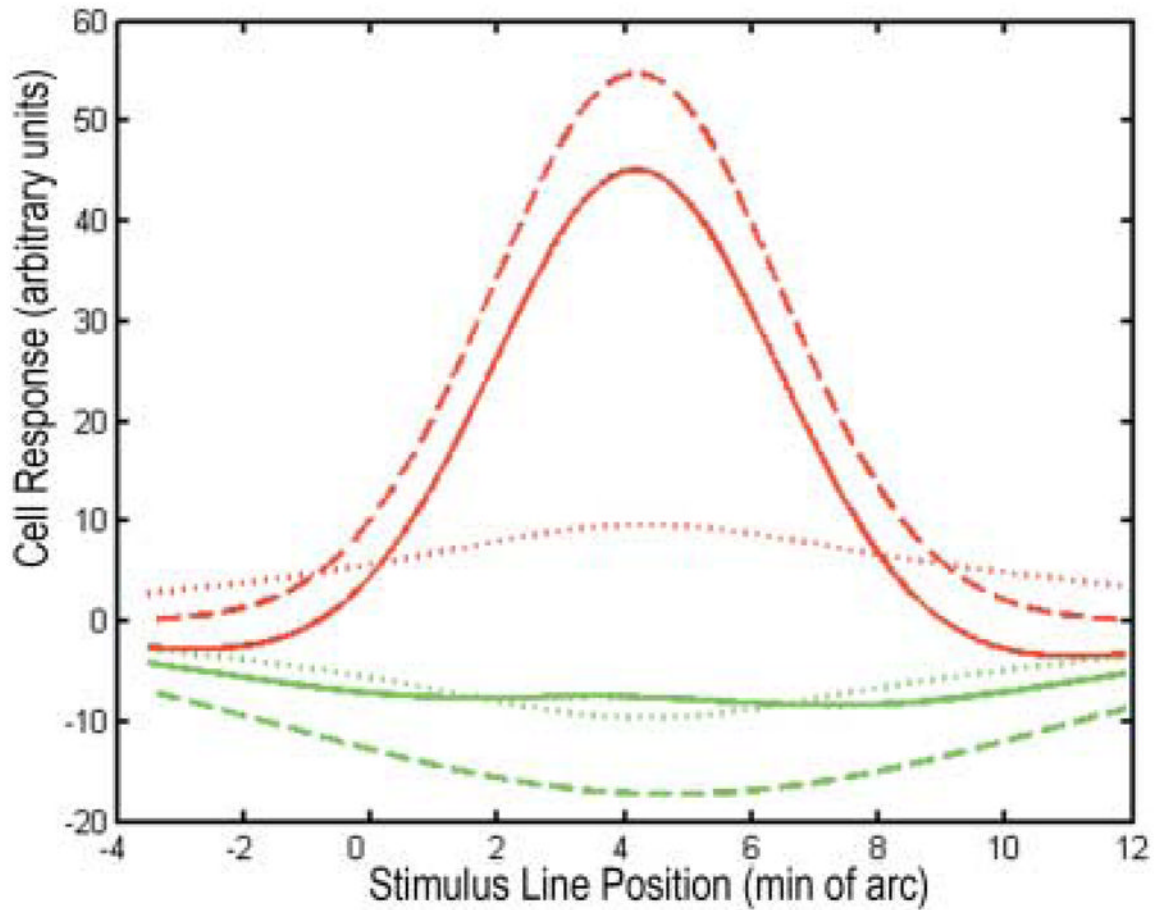
## References

- Abbott LF, Nelson SB. Synaptic plasticity: Taming the beast. *Nature Neuroscience*. 2000; 3:1178–1183.
- Benardete EA, Kaplan E. Dynamics of primate P retinal ganglion cells: Responses to chromatic and achromatic stimuli. *Journal of Physiology*. 1999; 519:775–790. [PubMed: 10457090]
- Boos R, Schneider H, Wässle H. Voltage- and transmitter-gated currents of All-amacrine cells in a slice preparation of the rat retina. *Journal of Neuroscience*. 1993; 13:2874–2888. [PubMed: 7687279]
- Boycott BB, Hopkins JM, Sperling HG. Cone connections of the horizontal cells of the rhesus monkey's retina. *Proceedings of the Royal Society B*. 1987; 229:345–379.
- Buzás P, Blessing EM, Szmajda BA, Martin PR. Specificity of M and L cone inputs to receptive fields in the parvocellular pathway: Random wiring with functional bias. *Journal of Neuroscience*. 2006; 26:1148–1161.
- Calkins DJ, Sterling P. Absence of spectrally specific lateral inputs to midget ganglion cells in primate retina. *Nature*. 1996; 381:613–615. [PubMed: 8637598]
- Calkins DJ, Schein SJ, Tsukamoto Y, Sterling P. M and L cones in macaque fovea connect to midget ganglion cells by different numbers of excitatory synapses. *Nature*. 1994; 371:70–72. [PubMed: 8072528]
- Calkins DJ. Seeing with S cones. *Progress in Retinal and Eye Research*. 2001; 20:255–287. [PubMed: 11286894]
- Callaway EM. Structure and function of parallel pathways in the primate early visual system. *Journal of Physiology*. 2005; 566:13–19. [PubMed: 15905213]
- Campbell FW, Gubish RW. Optical quality of the human eye. *Journal of Physiology*. 1966; 186:558–578. [PubMed: 5972153]
- Croner LJ, Kaplan E. Receptive fields of P and M ganglion cells across the primate retina. *Vision Research*. 1995; 35:7–24. [PubMed: 7839612]
- Dacey DM, Lee BB. The 'blue-on' opponent pathway in primate retina originates from a distinct bistratified ganglion cell type. *Nature*. 1994; 367:731–735. [PubMed: 8107868]
- Dacey DM, Packer OS. Colour coding in the primate retina: Diverse cell types and cone specific circuitry. *Current Opinion in Neurobiology*. 2003; 13:421–427. [PubMed: 12965288]
- Dacey DM. Primate retina: Cell types, circuits and color opponency. *Progress in Retinal and Eye Research*. 1999; 18:737–763. [PubMed: 10530750]
- Dacey DM, Lee BB, Stafford DK, Pokorny J, Smith VC. Horizontal cells of the primate retina: cone specificity without spectral opponency. *Science*. 1996; 271:656–659. [PubMed: 8571130]
- Dacheux RF, Raviola E. Physiology of H1 horizontal cells in the primate retina. *Proceedings of the Royal Society B*. 1990; 239:213–230.
- Dacheux RF, Chimento MF, Amthor FR. Synaptic input to the On-Off directionally selective ganglion cell in the rabbit retina. *Journal of Comparative Neurology*. 2003; 456:267–278. [PubMed: 12528191]
- Dan Y, Poo MM. Spike timing dependent plasticity of neural circuits. *Neuron*. 2004; 44:23–30. [PubMed: 15450157]
- Deeb SS, Diller LC, Williams DR, Dacey DM. Inter-individual and topographical variation of L:M cone ratios in monkey retinas. *Journal of the Optical Society of America A: Optics, Image Science and Vision*. 2000; 17:538–544.
- De Monasterio FM, Gouras P. Functional properties of ganglion cells of the rhesus monkey retina. *Journal of Physiology*. 1975; 251:167–195. [PubMed: 810576]
- Dowling JE, Boycott BB. Organization of the primate retina: Electron microscopy. *Proceedings of the Royal Society London B Biological Sciences*. 1966; 166:80–111.
- Hornstein HP, Verveij J, Schnapf JL. Electrical coupling between red and green cones in primate retina. *Nature Neuroscience*. 2004; 7:745–750.
- Jusuf PR, Martin PR, Grünert U. Synaptic connectivity in the midget-parvocellular pathway of primate central retina. *Journal of Comparative Neurology*. 2006; 494:260–274. [PubMed: 16320234]



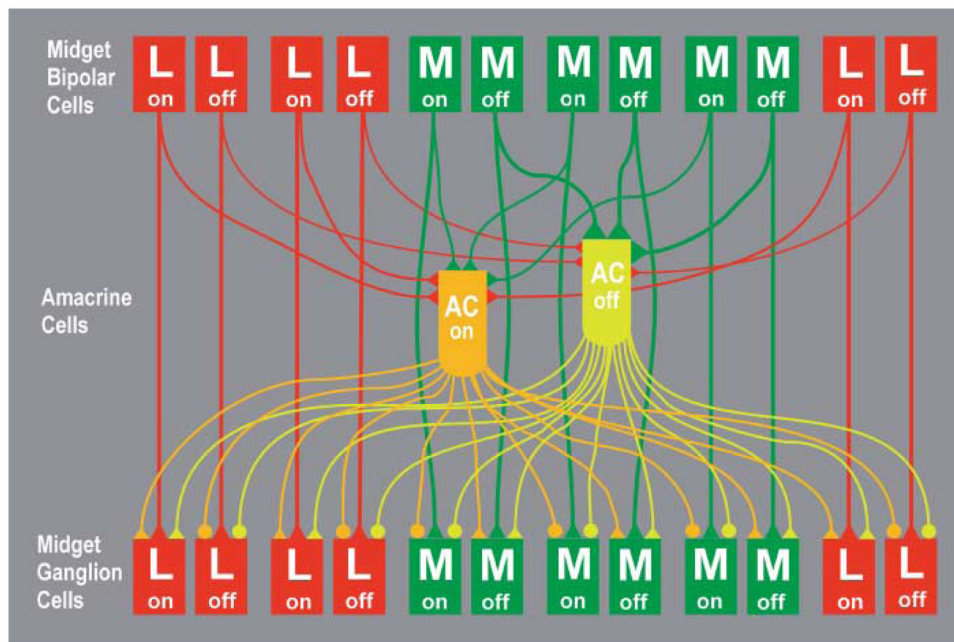
- Kaplan E, Purpura K, Shapley RM. Color and luminance contrast as tools for probing the primate retina. *Neuroscience Research*. 1988; 8:S151–S165.
- Klug K, Herr S, Ngo IT, Sterling P, Schein S. Macaque retina contains an S cone OFF midget pathway. *Journal of Neuroscience*. 2003; 23:9881–9887. [PubMed: 14586017]
- Kolb H, Dekorver L. Midget ganglion cells of the parafovea of the human retina: A study by electron microscopy and serial section reconstructions. *Journal of Comparative Neurology*. 1991; 303:617–636. [PubMed: 1707423]
- Kolb H, Linberg KA, Fisher SK. Neurons of the human retina: A Golgi study. *Journal of Comparative Neurology*. 1992; 318:147–187. [PubMed: 1374766]
- Kolb H, Marshak DW. The midget pathways of the primate retina. *Documenta Ophthalmologica*. 2003; 106:67–81. [PubMed: 12675488]
- Kolb H, Zhang L, Dekorver L, Cuenca N. A new look at calretinin-immunoreactive amacrine cell types in the monkey retina. *Journal of Comparative Neurology*. 2002; 453:168–184. [PubMed: 12373782]
- Koontz M, Hendrickson AE. Stratified distribution of synapses in the inner plexiform layer of primate retina. *Journal of Comparative Neurology*. 1987; 263:581–592. [PubMed: 3667989]
- Kouyama N, Marshak DW. Bipolar cells specific for blue cones in the macaque retina. *Journal of Neuroscience*. 1992; 12:1233–1252. [PubMed: 1556594]
- Lebedev DS, Marshak DW. Amacrine cell contributions to red-green opponency in central primate retina: A model study. *Perception*. 2006; 35:21.
- Lebedev DS. A computational model of the midget pathways in the central primate retina. *Sensory Systems*. 2003; 17:91–106. (In Russian).
- Lee, BB. Structure of receptive field centers of midget retinal ganglion cells. In: Mollon, JD.; Pokorny, J.; Knoblauch, K., editors. *Normal and Defective Colour Vision*. New York: Oxford University Press; 2003. p. 63-70.
- Lee BB, Kremers J, Yeh T. Receptive fields of primate retinal ganglion cells studied with a novel technique. *Visual Neuroscience*. 1998; 15:161–175. [PubMed: 9456515]
- Lee SCS, Grünert U. Connections of diffuse bipolar cells in primate retina are biased against S-cones. *Journal of Comparative Neurology*. 2007; 502:126–140. [PubMed: 17335043]
- Lee SCS, Telkes I, Grünert U. S-cones do not contribute to the OFF midget pathway in the retina of the marmoset, *Callithrix jacchus*. *European Journal of Neuroscience*. 2005; 22:437–447. [PubMed: 16045497]
- Lennie, P.; Haake, W.; Williams, DR. The design of chromatically opponent receptive fields. In: Landy, MS.; Movshon, JA., editors. *Computational Models of Visual Processing*. Cambridge, MA: MIT Press; 1991.
- Mariani AP. Amacrine cells of the rhesus monkey retina. *Journal of Comparative Neurology*. 1990; 15:382–400. [PubMed: 2262597]
- Martin PR, Lee BB, White AJ, Solomon SG, Rüttiger L. Chromatic sensitivity of ganglion cells in the peripheral primate retina. *Nature*. 2001; 410:933–936. [PubMed: 11309618]
- Marty A, Llano I. Excitatory effects of GABA in established brain networks. *Trends in Neurosciences*. 2005; 28:284–289. [PubMed: 15927683]
- Maximov PV, Marshak DW, Lebedev DS. A role for the blue pathway in the development of red green opponency. *Perception*. 2006; 35:195.
- McMahon MJ, Lankheet MJ, Lennie P, Williams DR. Fine structure of parvocellular receptive fields in the primate fovea revealed by laser interferometry. *Journal of Neuroscience*. 2000; 20:2043–2053. [PubMed: 10684905]
- Momiji H, Bharath AA, Hankins MW, Kennard C. Numerical study of short-term afterimages and associate properties in foveal vision. *Vision Research*. 2006; 46:365–381. [PubMed: 16297956]
- Momiji H, Hankins MW, Bharath AA, Kennard C. A numerical study of red-green colour opponent properties in the primate retina. *European Journal of Neuroscience*. 2007; 25:1155–1165. [PubMed: 17331211]
- Neitz J, Carroll J, Yamauchi Y, Neitz M, Williams DR. Color perception is mediated by a plastic neural mechanism that is adjustable in adults. *Neuron*. 2002; 35:783–792. [PubMed: 12194876]

- Packer OS, Dacey DM. Receptive field structure of H1 horizontal cells in macaque monkey retina. *Journal of Vision*. 2002; 2:272–292. [PubMed: 12678578]
- Passaglia CL, Troy JB, Ruttiger L, Lee BB. Orientation sensitivity of ganglion cells in primate retina. *Vision Research*. 2002; 42:683–694. [PubMed: 11888534]
- Reid RC, Shapley RM. Spatial structure of cone inputs to receptive fields in primate lateral geniculate nucleus. *Nature*. 1992; 356:716–718. [PubMed: 1570016]
- Rodieck RW. Quantitative analysis of cat retinal ganglion cell responses to visual stimuli. *Vision Research*. 1965; 5:583–601. [PubMed: 5862581]
- Roorda A, Metha AB, Lennie P, Williams DR. Packing arrangement of the three cone classes in primate retina. *Vision Research*. 2001; 41:1291–1306. [PubMed: 11322974]
- Shapley R, Reid RC, Kaplan E. Receptive fields of P and M cells in the monkey retina and their photoreceptor inputs. *Neuroscience Research*. 1991; 15:S199–S211.
- Smith EL 3rd, Chino YM, Ridder WH 3rd, Kitagawa K, Langston A. Orientation bias of neurons in the lateral geniculate nucleus of macaque monkeys. *Visual Neuroscience*. 1990; 5:525–545. [PubMed: 2085469]
- Smith VC, Lee BB, Pokorny J, Martin PR, Valberg A. Responses of macaque ganglion cells to the relative phase of heterochromatically modulated lights. *Journal of Physiology*. 1992; 458:191–221. [PubMed: 1302264]
- Solomon SG, Lennie P. The machinery of colour vision. *Nature Reviews Neuroscience*. 2007; 8:276–286.
- Solomon SG, Lee BB, White AJ, Ruttiger L, Martin PR. Chromatic organization of ganglion cell receptive fields in the peripheral retina. *Journal of Neuroscience*. 2005; 25:4527–4539. [PubMed: 15872100]
- Vu TQ, Payne JA, Copenhagen DR. Localization and developmental expression patterns of the neuronal KCl cotransporter (KCC2) in the rat retina. *Journal of Neuroscience*. 2000; 20:1414–1423. [PubMed: 10662832]
- Woodin MA, Ganguly K, Poo MM. Coincident pre and postsynaptic activity modifies GABAergic synapses by postsynaptic changes in Cl transporter activity. *Neuron*. 2003; 39:807–820. [PubMed: 12948447]

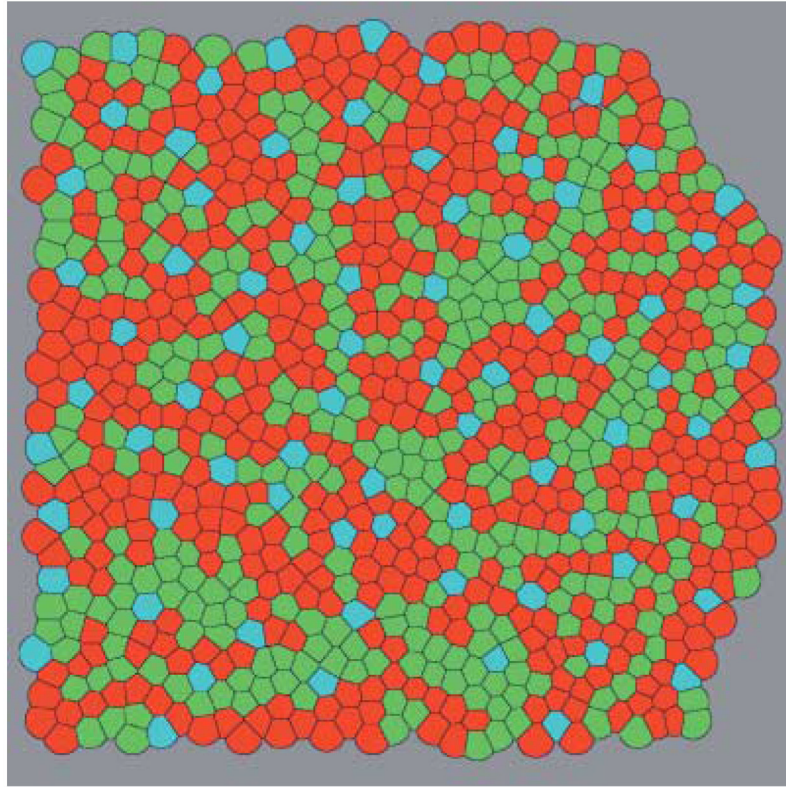


**Fig. 1.**

One dimensional receptive field profiles of a central midget ganglion cell with an L-ON center, approximated by the difference between two Gaussians. Red and green curves correspond to L and M cone-isolating stimuli, respectively. Each stimulus is a narrow straight line on a uniform background. Solid curves were generated as described in Eq. (1) (see text). The responses to L cone stimulation had negative-going components on either side of the peak, as predicted by the “mixed surround” hypothesis. Dashed curves were generated according to Eq. (2) with cone-specific surrounds. These correspond more closely to results of electrophysiological experiments with cone-isolating stimuli. Dotted curves depict the difference between curves (1) and (2), the hypothetical signals from amacrine cells.

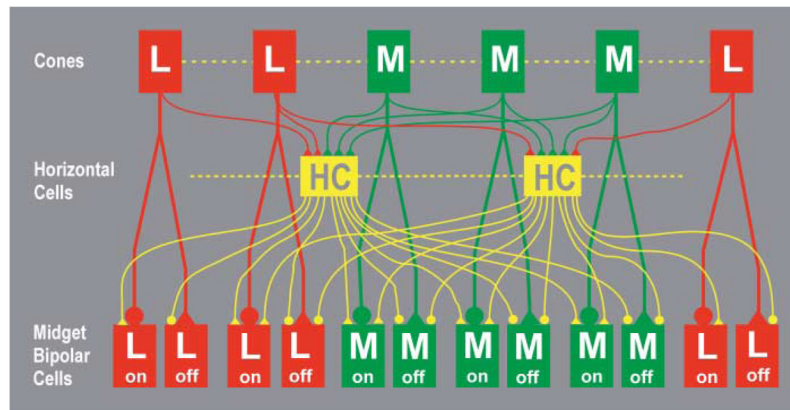


**Fig. 2.** The inputs and outputs of model amacrine cells (AC). The OFF amacrine cells (yellow-green) received sign conserving synapses (triangles) from both L OFF and M OFF midget bipolar cells. The synapses from M OFF bipolar cells were stronger and therefore are depicted with larger triangles. The ON amacrine cells (orange) received equally strong sign conserving inputs from L ON and M ON midget bipolar cells. The synapses from both types of amacrine cells onto L ON and M OFF midget ganglion cells were sign conserving, and the synapses from both types of amacrine cells onto L OFF and M ON were sign inverting (circles). A version for readers with red-green color blindness is available in Supplemental Materials Online.



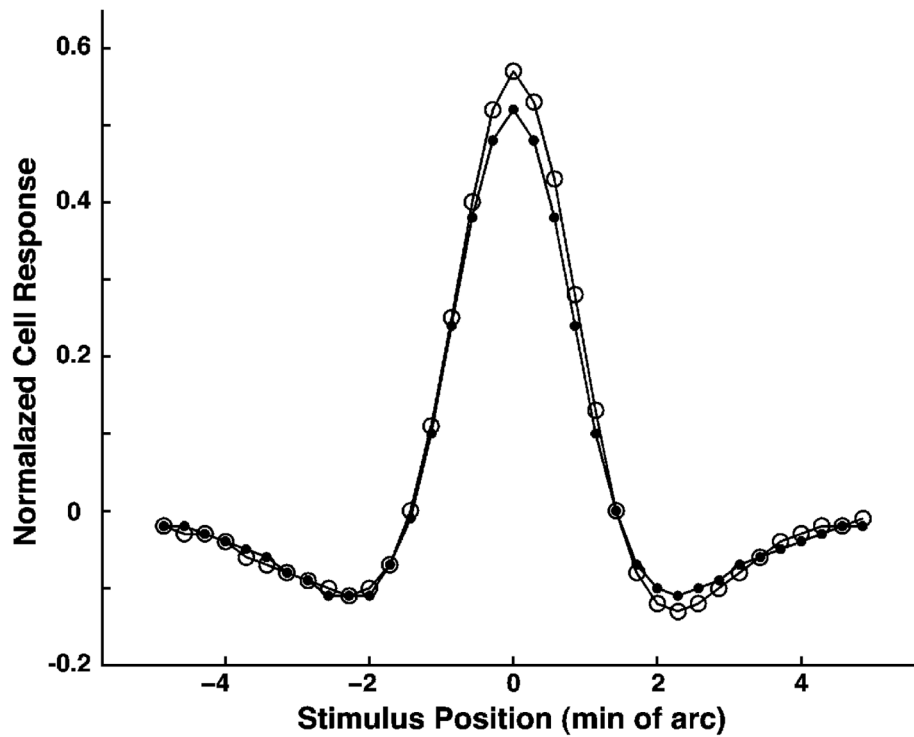
**Fig. 3.** The fragment of a cone mosaic from central macaque retina used for the model (Roorda et al., 2001). The cones are shown as Voronoi cells constructed around the cone center coordinates. L cones are red; M cones green and S cones blue. A version with all cones numbered is available in Supplemental Materials Online.



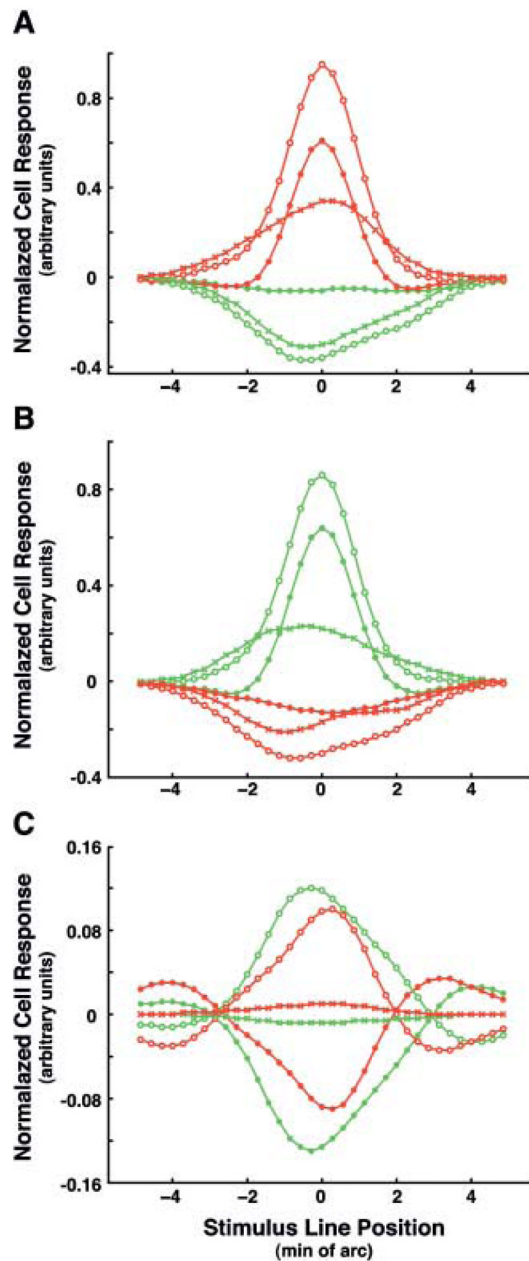


**Fig. 4.** The connections between cones, horizontal cells and bipolar cells in the model (Lebedev, 2003). Electrical coupling between L and M cones and between horizontal cells (HC) is indicated by dashed lines. Sign conserving synapses are indicated by triangles and sign inverting synapses by circles. Horizontal cells receive equal numbers of inputs from L and M cones and are depicted in yellow to indicate their lack of selectivity. Model midget bipolar cells each receive inputs from a single L or M cone. A version for readers with red-green color blindness is available in Supplemental Materials Online.



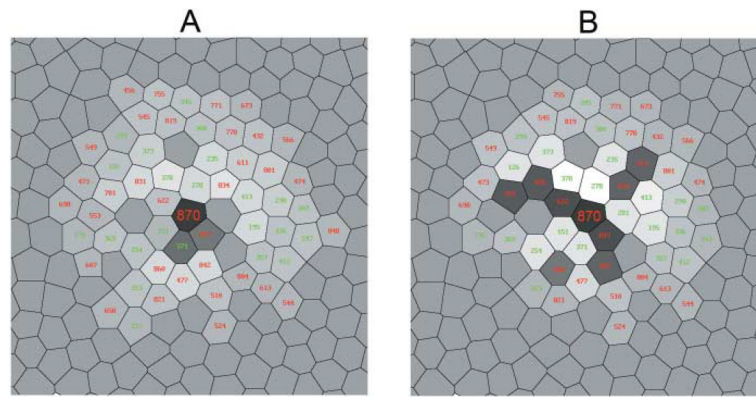


**Fig. 5.** One dimensional receptive field profiles of a model ganglion cell measured with an achromatic, straight line stimulus. The curve with open circles was generated with model amacrine cells active. The curve with smaller, closed circles was generated with model amacrine cell signals switched off. There was very little difference between the two sensitivity profiles, an indication that the model amacrine cells play a very small role in the steady state responses to achromatic stimuli.



**Fig. 6.** One-dimensional receptive field profiles of two model ON ganglion cells measured with cone specific straight line stimuli. Red and green curves correspond to L and M cone-isolating stimuli, respectively. The curves with open circles were generated with active model amacrine cells. The curves with closed circles depict the profiles with the amacrine cell signals switched off. The curves with Xs depict signals from the model amacrine cells. (A) The profiles for model ganglion cell #870 with an L ON center. (B) The profiles for model ganglion cell #413 with an M ON center. Note the negative going regions in both responses to stimulation of the central cone type without amacrine cells. (C) Fig. 6C illustrates the role of the model amacrine cells. The curves marked with open circles, red for L stimulus and green for the M stimulus, depict the summed signal of 4 ON and 4 OFF amacrine cells that provide input to model ganglion cell #870. A comparison of the peak

values shows the presence of a bias. The negative response of the OFF amacrine cell to the M stimulus is larger in absolute value than the positive response of the ON amacrine cell, and the opposite is true for the L stimulus. Curves with Xs depict the sums of ON and OFF signals for both the stimuli. These curves differ from similar curves in Fig 6A only by scale; this is attributable to slight differences in the amplification factors.

**Fig. 7.**

Fine structure of the receptive field of the model ON midget bipolar cell driven mainly by cone #870, an L cone, and its postsynaptic ON midget ganglion cell, measured with a point source of light illuminating a single cone at a time. The cell whose receptive field is illustrated is at the center of the diagram and is identified by large numbers. The chromatic type of each cone is indicated by the color of the number. The responses of the model midget bipolar cell and midget ganglion cell to the stimulation of each cone are indicated by the grey levels. The darker grays are positive (excitatory) values; the lighter grays and white are negative (inhibitory) values. An intermediate grey level indicates the cones, making no contribution to the response of the cell, in particular, all S cones. **(A)** The receptive field structure of the model bipolar cell postsynaptic to cone #870, which is equivalent in the model to the ganglion cell with amacrine cells switched off. **(B)** The receptive field structure of the model ganglion cell postsynaptic to that bipolar cell with active amacrine cells.

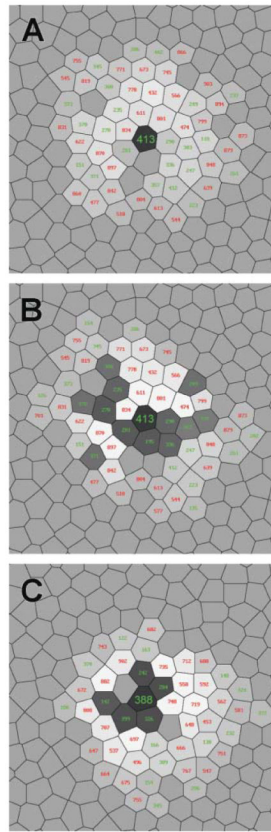


**Fig. 8.** The fine structure of the receptive fields of the ON midget bipolar cell (A) and ON midget ganglion cell (B) driven mainly by cone #413, an M cone. (C) The fine structure of the receptive field of the model M ON center ganglion cell receiving its primary input from cone #388. Conventions are the same as in Fig. 7.

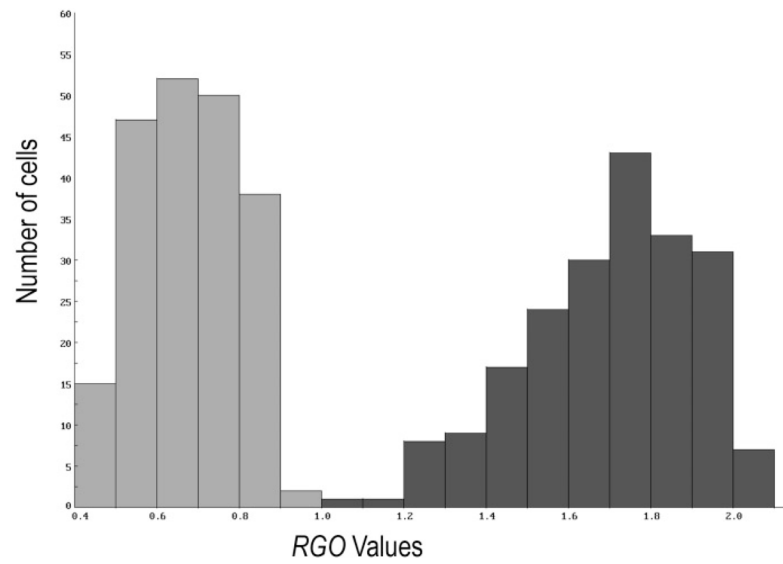


**Fig. 9.** Enhancement of red-green opponency, *RGO*, by the model amacrine cells. The left histogram (light grey) shows the measured *RGO* values for all the model ganglion cells when amacrine cells are switched off, and the right histogram (dark grey) shows the results with active amacrine cells.



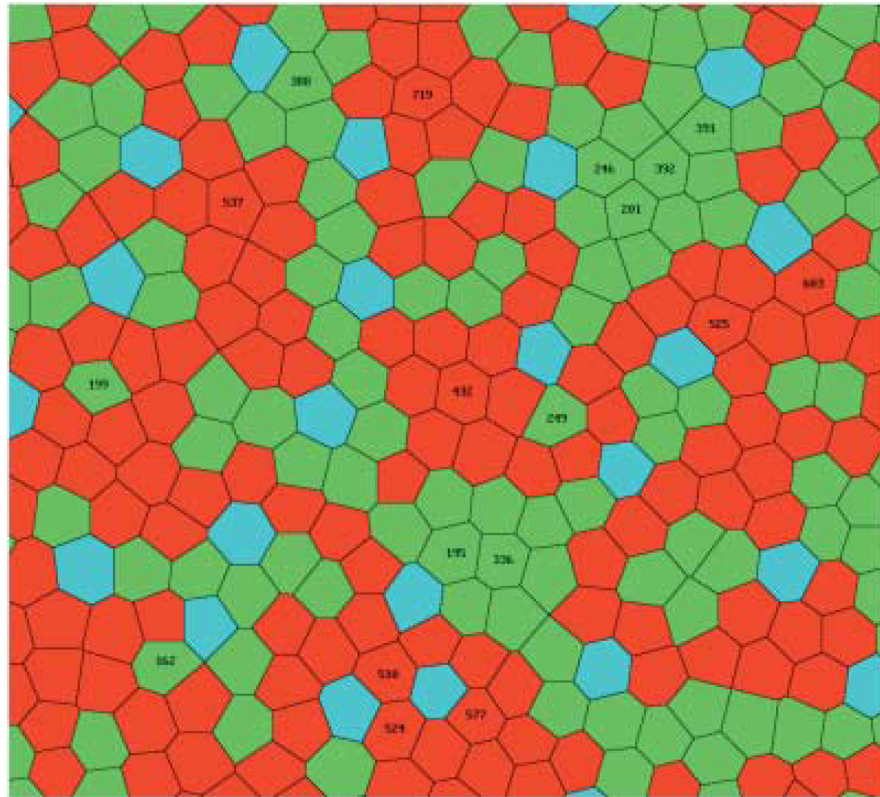


**Fig. 10.** The central part of the cone mosaic fragment. The 18 midget ganglion cells marked with black digits have different values of *RGO*. L cone #748, marked with white digits, is a nearest neighbor of the M cone #388 (see text).

**Table 1**

RGO values of 18 model ganglion cells. In the first column the numbers of the central cones according to Roorda et al. (2001) are shown. The RGO values are in the second column. The third column depicts the ganglion cell ranking, the position in the list of 204 ganglion cells ordered by RGO values. In the fourth column the types of the central and surrounding cones are presented. For example, L/2L+3M+S means that the corresponding ganglion cell has an L cone center at its receptive field center and 2, 3 and 1 surrounding cones of L, M and S type, respectively. The complete dataset is available in Supplemental Materials Online

Cell number	RGO	Ranking	Center/Surr.	Cell number	RGO	Ranking	Center/Surr.
524	1.09	1	L03L3M32S	336	1.63	68	M06M
392	1.11	2	M06M	195	1.68	87	M05M3S
246	1.26	6	M05M3S	162	1.71	96	M05L3S
577	1.32	12	L05L3S	537	1.72	103	L06L
391	1.33	14	M05M3S	249	1.73	111	M05L3S
510	1.40	19	L04L32S	719	1.74	115	L06L
201	1.45	25	M06M	525	1.86	158	L05L3S
432	1.52	43	L06L	388	2.04	203	M0L34M3S
199	1.61	64	M06L	603	2.05	204	L04L3M3S